Corrosion Science **55**, 97-106 (2011), doi:10.1016/j.corsci.2011.10.006

Influence of the Composition of Working Fluids on Flow-Accelerated Organic Coating Degradation:

Deionized Water versus Electrolyte Solution

Qixin Zhou [a], Yechun Wang [a,*], Gordon P. Bierwagen [b]

a: Mechanical Engineering, North Dakota State University, NDSU Dept. 2490, PO Box 6050, Fargo, North Dakota, 58108 USA

b: Coatings and Polymeric Materials, North Dakota State University, NDSU Dept. 2760, PO Box 6050, Fargo, North Dakota, 58108 USA

*: Corresponding author. Tel: +1-701-231-6732; Fax: +1-701-231-8913;

E-mail address: yechun.wang@ndsu.edu

Abstract

Corrosion protective coatings are known to degrade due to moisture exposure. To predict coatings service lifetime, acceleration tests are necessary. We employ flowing deionized water to accelerate coating degradation. Coating barrier properties are found, via Electrochemical Impedance Spectroscopy (EIS), to decrease as flow rate (Q) increases, similar to findings for coatings in NaCl solution. EIS modulus decreases more for coatings in deionized water than those in electrolyte solution. Topographical characterizations show severe coating blistering in deionized water immersion with higher Q, but not in electrolyte solutions. Deionized water is thus believed to accelerate more aggressively the degradation than electrolyte solution.

Keywords

A. Organic coatings; B. Electrochemical Impedance Spectroscopy;

1. Introduction

Organic coatings perform two primary functions: protection and decoration [1]. Applying organic coatings is the most common and usually the most cost effective approach to protect metallic objects and structures against corrosion [2]. Organic coatings act as barriers providing resistance to the transportation of oxygen, water and ions to the coating metal interface, and hence limiting corrosion [3].

Accelerated exposure tests are effective in predicting the service lifetime and assessing the quality of organic coatings. These tests are especially useful for good coating systems since the true field performance lifetime data is time-consuming and expensive to acquire [4]. The goal of accelerated exposure tests for corrosion protective coatings is to impose a repeatable and measurable set of stresses to the coating metal system similar, but in excess of the stresses the coating faces in field use. These excess stresses ideally cause the system to fail faster than it normally would, but the mechanism of failure remains the same as in the non-accelerated conditions [4, 5]. This is the requirement for all true accelerated exposure tests. Existing accelerated tests for organic coatings include salt fog chambers, QUV test, thermal cycling test, cyclic wet-dry test, etc. [5-10]. The accelerating approaches may alter the failure mechanism or require a long exposure time. For example, salt fog or Prohesion requires as much as 2000h exposure to qualitatively differentiate coating samples [5]. High performance coatings may need over a year of accelerated exposure. A more efficient acceleration test which preserves the coating failure mechanism at the same time is thus needed for more rapid service lifetime prediction of protective organic coatings.

Flow induced corrosion is complicated, since flow velocity, flow pattern, solid particles, and impact angles all contribute to the corrosion process [11-18]. Heitz [19] classified four types of mechanisms to describe the conjoint action of flow and corrosion. They are mass transport controlled corrosion, phase transport controlled corrosion, erosion corrosion and cavitation

corrosion. Many researches focus on studying erosion corrosion regimes so as to reveal the internal mechanism of the flowing corrosion [15, 18, 20-24]. A plethora of studies has been conducted for flow induced un-coated metal corrosion [12-17, 20-22] while the influence of flow over organic coatings has received less attention. Some work [25] mentioned that the hydrodynamic descriptions are difficult for the coating-metal system because a multitude of fluid-wall interactions can take place in the protective layer. These interactions include mass transfer, heat transfer, fluctuating shear stresses parallel to the surface, fluctuating energy densities perpendicular to the surface, particle impact and near wall gas bubble collapse.

Traditionally, investigations on the degradation of organic coatings are performed for coatings immersed in stationary solutions [26-28]. Recently, more attention has been paid on flowing solution over the organic coatings. Jeffcoate and Bierwagen [29] initially reported that the flowing electrolyte has a marked effect upon the performance of a coating system. Wei, Zhang and Ke [30] studied the degradation of epoxy powder coating under flowing and static immersion condition in 3% NaCl solution. A rotating cylinder apparatus was employed to generate the flowing field. Le Thu, Bierwagen, and Touzain reported degradation behaviors of three different organic coatings under laminar flow [3]. However, the flow rate is not correlated with the coating degradation in the afore-mentioned studies. To our knowledge, the only work which relates varying flow rates with the degradation of organic coatings was conducted by Wang and Bierwagen [31]. They concluded that barrier properties of the coating decrease exponentially with the increasing flow rate of a 3.5 wt% NaCl solution and proposed that the flowing electrolyte solution could be used in acceleration tests for the service lifetime prediction of organic coatings.

The goal of this study is to improve the understanding of the performance of organic coating under different flow rates of different solutions, since recent work has proved that flow conditions accelerate coating degradation [29, 31]. Deionized (DI) water has been used as the working fluid in this study. Experimental results are compared with the previous study [31] in which a 3.5 wt% NaCl solution has been used as the working fluid. Electrolyte solutions are often adopted in

corrosion studies while most published studies using pure water (e.g. deionized or distilled water) are only for metallic materials [32-35]. This study first presents and compares the influence of two different working fluids (DI water versus NaCl solution) on organic coating degradation as characterized by Electrochemical Impedance Spectroscopy (EIS) measurements as the main approach. EIS has been considered as a valuable and powerful tool to assess the degradation of organic coatings [3, 27, 28, 31, 36, 37]. EIS has long been used to predict the service lifetime of corrosion protective coatings, rank the coatings systems, and measure the water uptake in coatings. EIS data are also assimilated to develop meaningful models to analysis the physical behavior of the coating degradation. Thus, equivalent circuit modeling is developed to interpret the EIS spectra. In addition, the topological changes of the coating surface are characterized as the degradation is accelerated by flowing fluid.

2. Experimental Method

2.1 Sample Preparation

Stainless steel panels (Q-Panel Lab Products, Cleveland, OH) are cut into 76 × 76 mm and used as the metal substrate. The panels are then pretreated by abrasion with sand paper and cleaned with hexane before coatings are applied. Before the abrasion, the gloss value of the stainless steel panels at angles of 20˚, 60˚ and 85˚ are 22.4 ± 4.3, 32.1 ± 3.8, and 13.7 ± 1.2, and after the abrasion those values become 26.3 ± 5.1, 75.6 ± 8.3 and 58.3 ± 10.7. The organic coatings used in this study are Korabor Aluminum Primer RP140 and Korethan Topcoat UT6581 (graciously supplied by KCC Corporation, Seoul, South Korea). The primer is a chlorinated rubber based coating with aluminum flake pigment. The topcoat is a polyurethane resin based finish coat. The liquid paints are applied by air spraying and cured in room temperature for 24 hours.

2.2 EIS Measurements

The experiment setup is adopted and modified from our previous study [31] as shown in Fig. 1. The working fluid is pumped from the fluid reservoir to the test section, and then recycled back to the reservoir. A rotameter maintains the flow rate at 3.683 cm^3/s and 5.233 cm^3/s, respectively. The temperature is controlled at 25˚C by a water bath and a temperature controlling system. A flow channel is constructed with plastic sheets. Coated stainless steel panels are adhered to the upper and lower channel walls. The flowing fluid goes through the gap between the two panels facing each other. The platinum meshes are embedded through the plastic plate to the upper channel wall acting either as counter electrodes or the reference electrode. Details of the flow channel setup can be found in Fig. 2 of Ref. [31]. Meanwhile an O-ring glass electrochemical cell with a traditional three-electrode setup is used in the stationary immersion test. Details of the setup could be found from the product notes of Gamry's PTC1 Paint Test Cell. DI water is adopted as the working fluid for both flowing and stationary immersion.

The three-electrode EIS setup is employed for all measurements in this study. For coatings immersed in flowing fluids, the electrochemical cell is composed of a stainless steel panel acting as the working electrode, a pair of platinum meshes, on the left and right sides of the test panel, acting as the counter electrode, and another platinum electrode, near the fluid outlet, acting as the reference electrode. For the stationary immersion, a saturated calomel electrode is employed as the reference electrode. The stainless steel panel and a platinum mesh are worked as the working and counter electrode, respectively. The measuring equipment is Reference 600 Potentiostat by Gamry Instruments. Measurements are taken over a frequency range of 10^{-2} to 10^5 Hz with ten points per decade using 15 mV rms AC. EIS measurements are carried out twice a day during a 30-day immersion period.

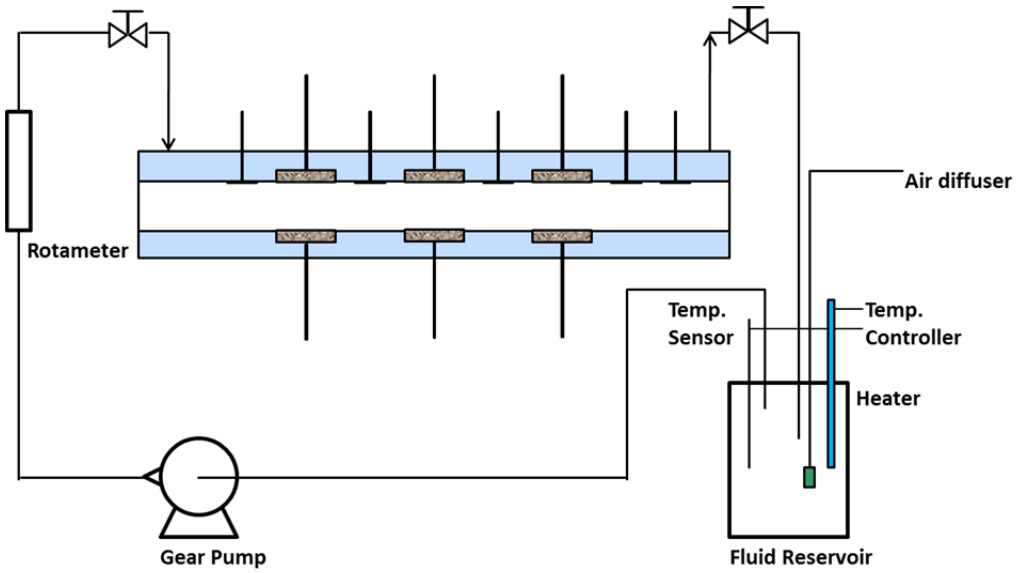

Fig. 1. Schematic diagram of the circulating flow.

2.3 Topography Characterization

Coating thickness and gloss are measured using an Elcometer coating thickness gauge and a NovoTrio statistical glossmeter before and after the immersion, respectively. The average thickness of dry coatings is 48 ± 5 μm in the experiment. An Axiovent 40 MAT (Focus Precision Instrument) is used for optical microscopy test. All images are collected over a magnification of 10X and 20X, depending on the features present on a given sample.

3. Results and Discussion

3.1 EIS Measurements

To characterize the barrier properties of organic coatings, EIS data are collected for coating samples immersed in the flowing and stationary DI water. As shown in Fig. 2 (a) for stationary immersion, the impedance modulus |Z| is plotted as a function of the frequency in EIS tests as well as the immersion time. Similar figures for samples immersed in flowing DI water at flow rates of Q=3.683 cm^3/s and Q=5.233 cm^3/s are presented in Fig. 2 (b) and (c), respectively.

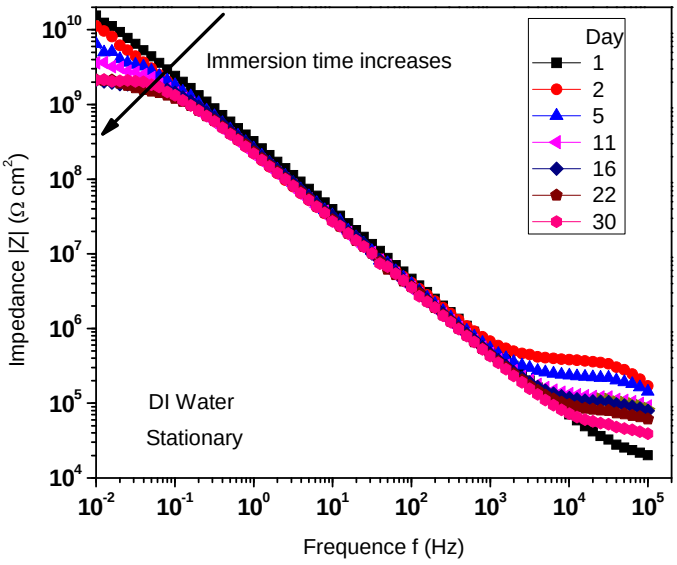

(a) Stationary DI water

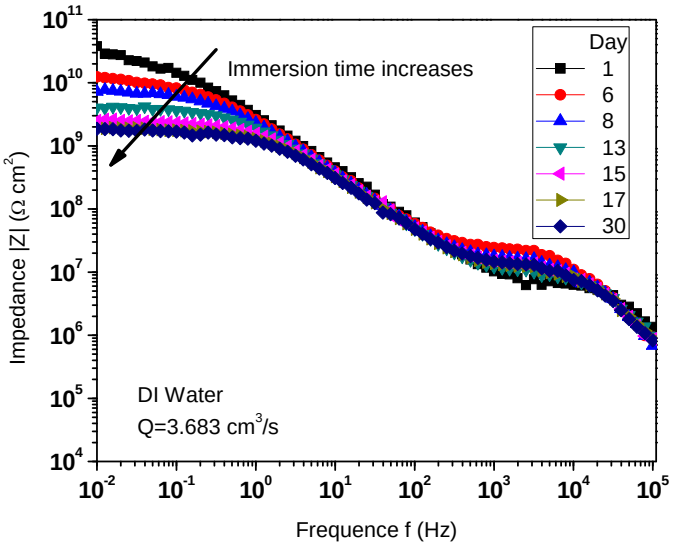

(b) Flowing DI water with Q=3.683 cm^3/s

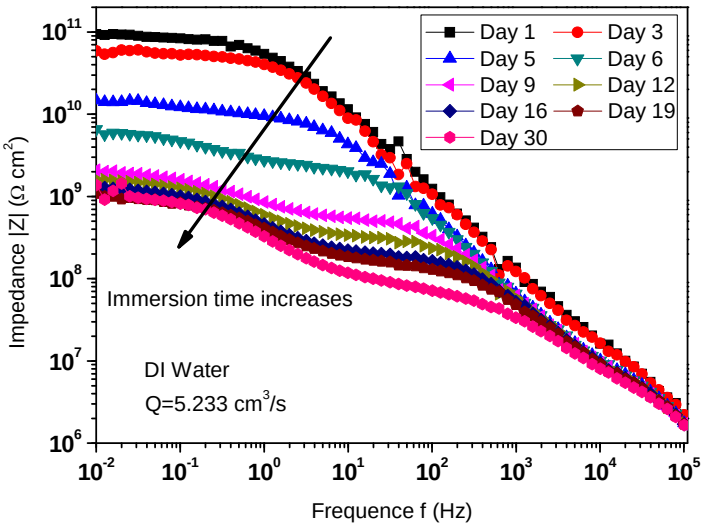

(c) Flowing DI water with Q=5.233 cm^3/s

Fig. 2. Impedance modulus as a function of frequency for coated samples immersed in DI water with flow rates Q=0 (stationary), 3.683 and 5.233 cm^3/s.

For all flow rates, the impedance modulus decreases with the immersion time, showing a loss of protective properties of the coatings. Due to the good quality of the coating samples which have no pinholes or air bubbles, the decrease of impedance modulus mainly indicates water uptake into the coating layer. The nonlinear behavior of the impedance modulus at higher frequencies could be the response of DI water contributing to EIS spectra, since the solution resistance may affect the Bode plot of EIS. Cottis and Turgoose mentioned in Chapter 4 of the book "Electrochemical Impedance and Noise" [38] that if the solution resistance is very small the impedance modulus linearly decreases as the frequency increases at high frequencies of the Bode plot, however, if the solution resistance is large and not negligible (e.g. DI water), nonlinear behavior is observed at high frequencies. (Please refer to Fig. 4.3 on page 37 of the Ref. [38].) We also measured the electrochemical impedance of DI water itself by EIS method using a three-electrode cell [39]. Platinum meshes are used as working and counter electrode. A saturated calomel electrode is used as the reference electrode and placed in the middle between the working and the counter electrode. The range of the measured impedance modulus is from 10^3 to 10^5 Ω. Hence the DI water is believed to have a high resistance which is not negligible [40]. In the afore-

mentioned measurement, the modulus is found to be independent on the frequency at mid-to-high frequencies. In addition, the nonlinear behavior at high frequencies of EIS spectra is also observed in literature [3, 41, 42] for other working fluids.

The impedance modulus at low frequency serves as a strong indicator of the corrosion resistance of coating samples [5]. To illustrate the change in the coating's barrier property over time, a plot of the relative low-frequency (0.01 Hz) impedance modulus as a function of time is shown in Fig. 3. The relative low-frequency impedance modulus is obtained by normalizing the low-frequency impedance modulus with the modulus at initial immersion. The decrease rate of relative low-frequency impedance modulus is substantial at the early stage of immersion followed by a relatively slower decrease. The decrease is more pronounced for flowing DI water than stationary immersion. Moreover, higher flow rates of the DI water further accelerates the decrease of the low-frequency impedance modulus. The high decrease rate reveals the flowing fluid enhances the water permeation into the coating metal interface, thus the process of organic coating degradation is accelerated by the flowing fluids. Similar behavior of the barrier properties (reflected via low-frequency impedance modulus) of the coatings was reported by Wang and Bierwagen [31] for coating samples immersed in NaCl solution with a variety of flow rates.

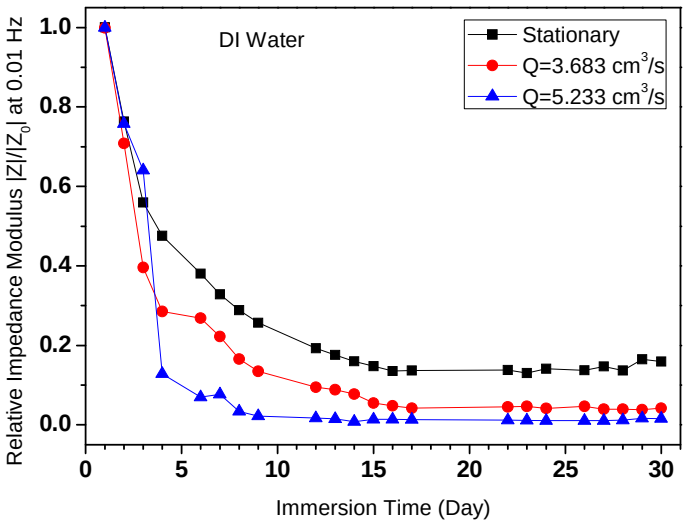

Fig. 3. Relative impedance modulus as a function of immersion time for coated samples immersed in DI water with flow rates Q=0 (stationary), 3.683, and 5.233 cm^3/s.

In order to compare the influence of different working fluids, the relative low-frequency impedance modulus of coatings immersed in DI water is compared with that in a 3.5 wt% NaCl solution. Comparison results are presented in Fig. 4 (a, b, c) for three different flow rates. For all cases, coatings immersed in NaCl solution show more abrupt decrease in its impedance modulus at initial immersion (up to 5-7 days) while the long-term decrease is more substantial for coatings immersed in DI water. We observe that for a 30-day immersion period the decrease in the barrier property of coatings is more substantially accelerated by flowing DI water than the NaCl solution.

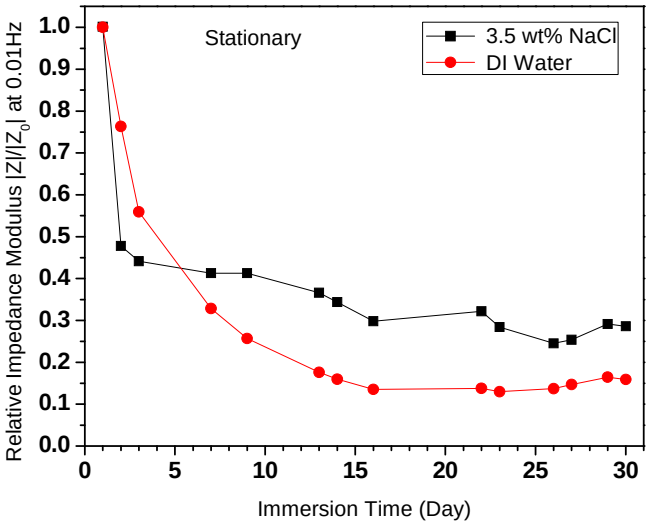

(a) Stationary immersion

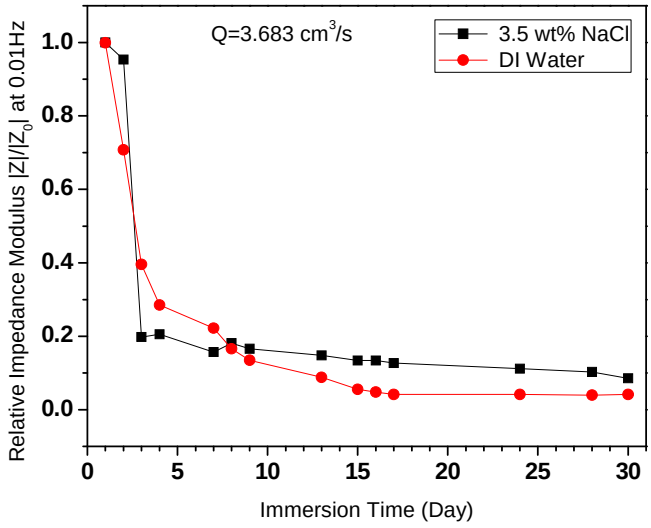

(b) Q=3.683 cm^3/s

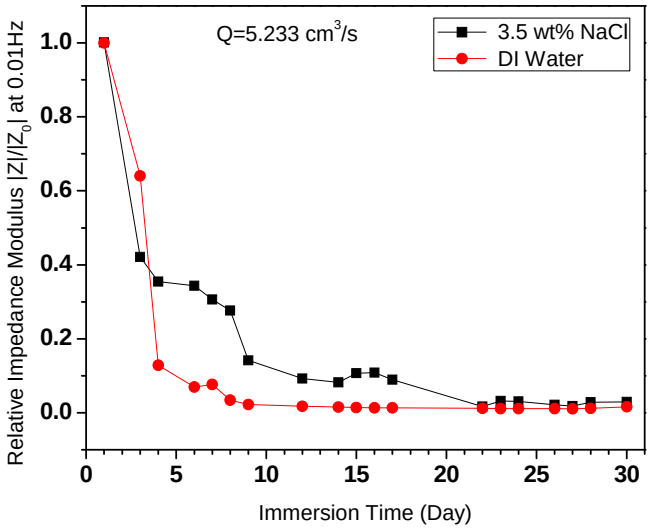

(c) Q=5.233 cm^3/s

Fig. 4. Relative impedance modulus as a function of immersion time for coated samples immersed in 3.5 wt% NaCl solution and DI water for flow rates Q=0 (stationary), 3.683, and 5.233 cm^3/s.

3.2 Equivalent Circuit Modeling

An equivalent circuit model as shown in Fig. 5 has been employed to analyze the physical behavior of coatings as they are degrading. In this study, software Zview is employed to fit model elements (i.e. solution resistance R_s, charge transfer resistance R_{ct} and constant phase element CPE) with the EIS spectra. A constant phase element (CPE) is used in the circuit to take into consideration the non-ideal capacitance behavior of the coating. Mathematically, a CPE impedance (Z_{CPE}) is given by [15],

$$Z_{CPE} = (j\,\omega)^{-p}/T$$

where ω is the angular frequency, T and p are constants and we refer to them as CPE-T and CPE-P respectively for the rest of this work. CPE-T stands for the coating capacitance and CPE-P is the exponent of the constant phase element. Generally, 0<CPE-P<1; when CPE-P=1 and CPE-T=C, the CPE behaves like an ideal capacitor with capacitance C; and when CPE-P=0, a resistance is represented. In this model, CPE element is in parallel with the charge transfer

resistance (R_{ct}). The solution resistance (R_s) is also included since different working fluids are employed.

Fig. 6 shows the relative values of the phase elements CPE-T and CPE-P as well as the charge transfer resistance R_{ct} as a function of immersion time under flowing and stationary DI water immersion. The relative values are obtained by normalizing the element values with those at the initial immersion. The values for impedance modulus |Z|, CPE-T, CPE-P and R_{ct} at initial immersion are listed in Table 1. In coating study, it is impossible to perform different acceleration tests on the same sample. Hence, in sample preparations we try to spray the coating substrate in exactly the same approach at the same time to ensure those samples to have approximately very similar properties. In this work, we have chosen to analyze a group of samples with the closest initial conditions. Thus, the initial values for individual parameters in different immersion tests are at the same order of magnitude with slight deviations from each other (as shown in Table 1). We observe an exponential increase of the coating capacitance (CPE-T) for the larger flow rate; while for the stationary and lower flow rate immersion CPE-T increases slowly and gradually approaches to a plateau. The constant phase element exponent (CPE-P) decreases during the immersion, more with the decrease larger for larger flow rates. The decrease in CPE-P implies the organic coating has no longer exhibited as an ideal capacitor after 30 days of flowing immersion [15, 28]. For example, the absolute value of CPE-P drops from 0.9238 to 0.3838 for coatings immersed in the flowing DI water with flow rate of Q=5.233 cm^3/s. The charge transfer resistance (R_{ct}) shows a rapid decrease initially and then maintains relatively constant during the immersion period for all cases. A larger flow rate causes a more substantial decrease for R_{ct}.

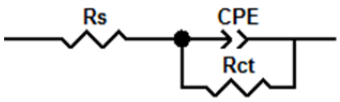

Fig. 5. Equivalent circuit model used for the impedance analysis of coated samples immersed in 3.5 wt% NaCl solution and DI water.

The increase of coating capacitance and decrease of resistance during immersion implies coating degradation occurs. An ideal capacitance behavior is obtained for excellent coatings [3]. When substrate is exposed to an aggressive environment, development of a resistive behavior is employed to indicate that degradation has occurred [3]. The capacitance evolution is usually related to the penetration of water, oxygen and ions into the coating, and generally, its value is expected to increase with the immersion time. Water permeation results in the increase of the relative permittivity of the entire coating system and attenuation of the barrier property of organic coatings. The behavior of the equivalent circuit elements in Fig. 6 shows that the coatings immersed in DI water flowing with a higher flow rate tends to experience more severe penetration of water, fluid shear abrasion and attenuation of coatings barrier properties. The results are qualitatively in agreement with the findings by Wang and Bierwagen [31] although a different working fluid was employed.

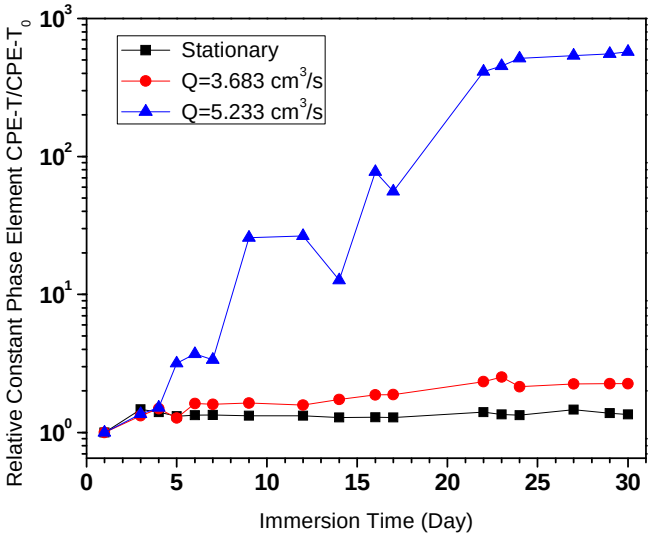

(a) CPE-T

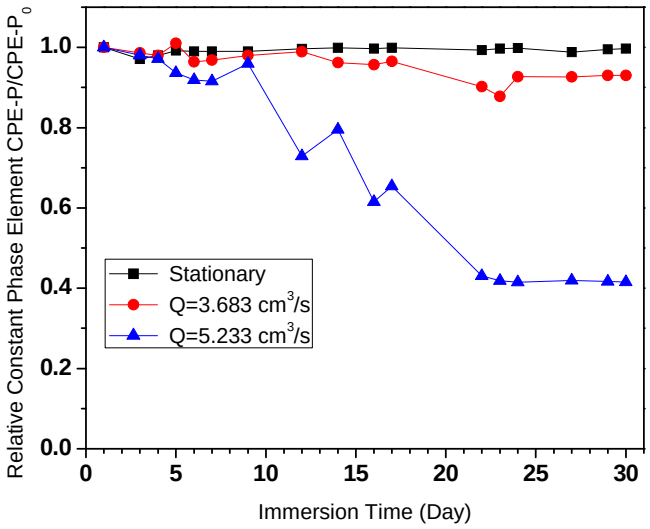

(b) CPE-P

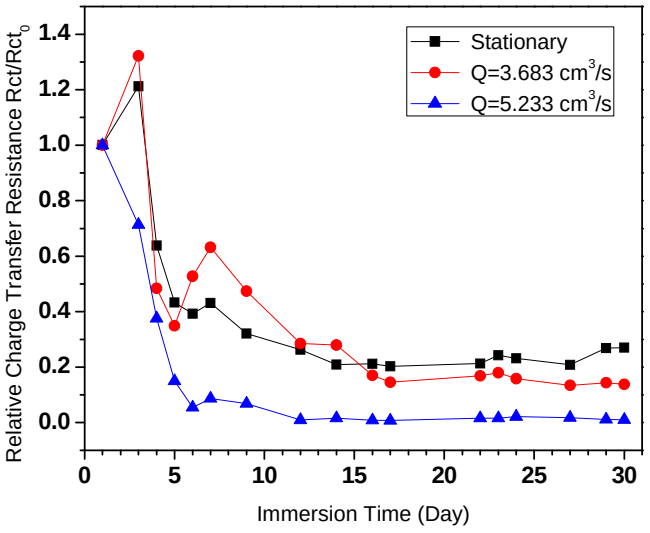

(c) R_{ct}

Fig. 6. Equivalent circuit model elements as a function of immersion time for coated samples immersed in DI water for flow rates Q=0 (stationary), 3.683, and 5.233 cm^3/s.

Results for the equivalent circuit modeling are compared with those from 3.5 wt% NaCl, the original EIS data of which is taken from Ref. [31]. The same model has been employed to analyze the data for the 3.5 wt% NaCl solution. Note that the solution resistance is 10 ~ 20 Ω and about 10^4 Ω for samples in the 3.5 wt% NaCl solution and the DI water, respectively. The resistance of the solution itself is also measured by three-electrode cell of the EIS test. The actual values for simulations of different samples may be slightly adjusted by the Zview software in

order to obtain a better fitting. Comparisons are shown in Fig.7 - 9 for different model elements at three flow rates.

As shown in Fig. 7, the coating capacitance (reflected as CPE-T) of coatings immersed in DI water shows greater increase over the entire immersion time than that in the NaCl solution for all flow rates (Q=0, 3.863, 5.233 cm^3/s). Since the relative permittivity of water (80.4 at 20˚C) is much higher than that of organic coatings (usually between 2 and 8), the water uptake causes an increase of the relative permittivity of the entire coating system so as to increase of the coating capacitance. Meanwhile we know (as a reference) that the relative permittivity of the 3.5 wt% NaCl solution is about 74.0 at 20˚C [43], which is slightly lower than that of the DI water. The existence of chloride ion in coating layers may lower the relative permittivity of the percolating fluid in the coating [43]. This may explain in part the fact that the coating capacitance shows higher values in DI water. We believe NaCl solution may exist in the coating layers due to the percolation of water and the diffusion of ions into the coating [7, 9, 44-46], although the concentration may not be exactly 3.5 wt%. The energy dispersive X-ray (EDX) and X-ray photoelectron spectroscopy (XPS) test have been used to confirm the presence of chloride element on the interface of the coating and substrate due to the diffusion of Cl^- from the solution [7, 44].

The advantage of using relative values such as Fig. 7 is that it demonstrates well the changes taking place in CPE-T over time and discounts the influence of the absolute values for different coating samples in different working fluids. Hence, we are able to conclude that the increase of coating capacitance is more pronounced in flowing conditions. We also notice that the difference in the evolution of relative CPE-T between the two working fluids is more prominent for higher flow rates. The barrier properties of the organic coatings are reduced earlier and rather severe by the flowing DI water immersion.

Fig. 8 shows the transient behavior of the relative values of CPE-P for coatings immersed in DI water as well as those in the NaCl solution. The decrease in CPE-P is more substantial for

coatings in DI water immersion, especially for higher flow rates. A similar behavior is also observed for the charge transfer resistance R_{ct} as shown in Fig. 9. DI water incurs a more substantial decrease in R_{ct}; greater difference in R_{ct} between the DI water and 3.5 wt% NaCl occurs for higher flow rates.

Table 1. Initial values of parameters for coating samples immersed in DI water

Parameters	Stationary	Q=3.683 cm^3/s	Q=5.233 cm^3/s
$\|Z\|$ (Ω cm^2)	1.56×10^{10}	3.80×10^{10}	8.44×10^{10}
CPE-T (F)	2.86×10^{-9}	3.14×10^{-9}	5.73×10^{-9}
CPE-P	0.9458	0.9128	0.9238
R_{ct} (Ω)	1.09×10^{9}	1.86×10^{9}	5.46×10^{9}

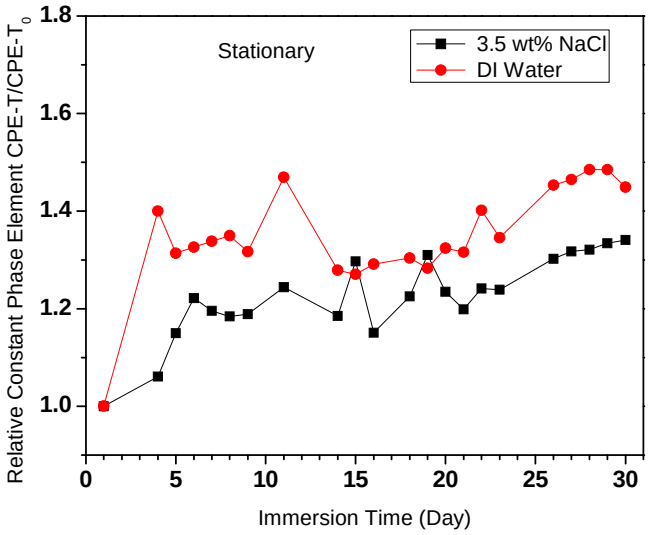

(a) Stationary immersion

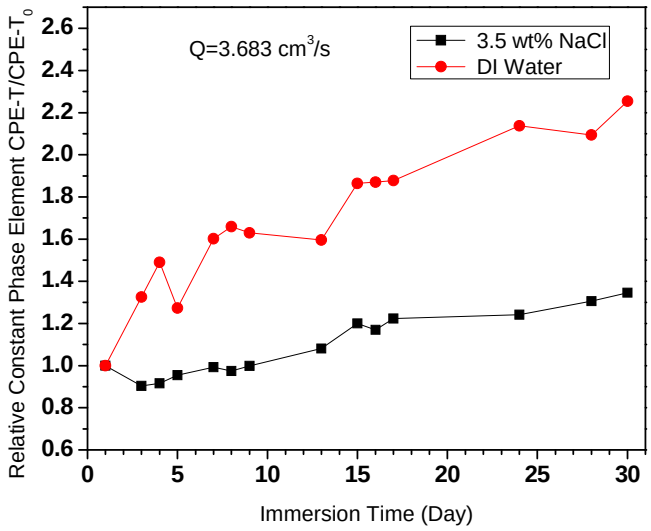

(b) Q=3.683 cm^3/s

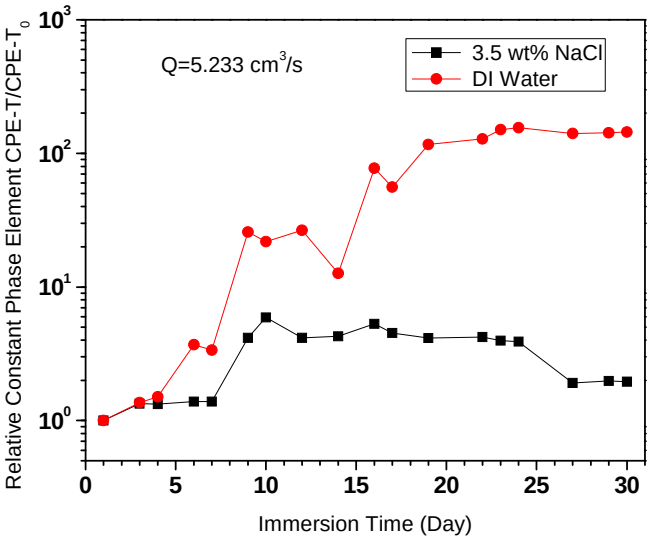

(c) Q=5.233 cm^3/s

Fig. 7. Relative constant phase element CPE-T as a function of immersion time for coated samples immersed in 3.5 wt% NaCl solution and DI water for flow rates Q=0 (stationary), 3.683, and 5.233 cm^3/s.

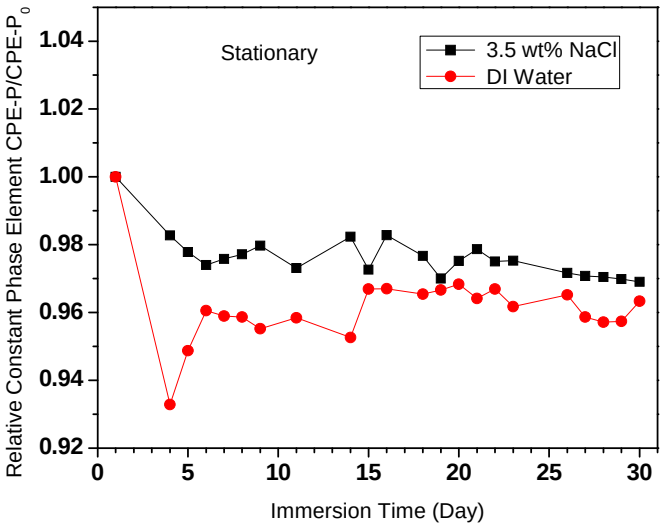

(a) Stationary immersion

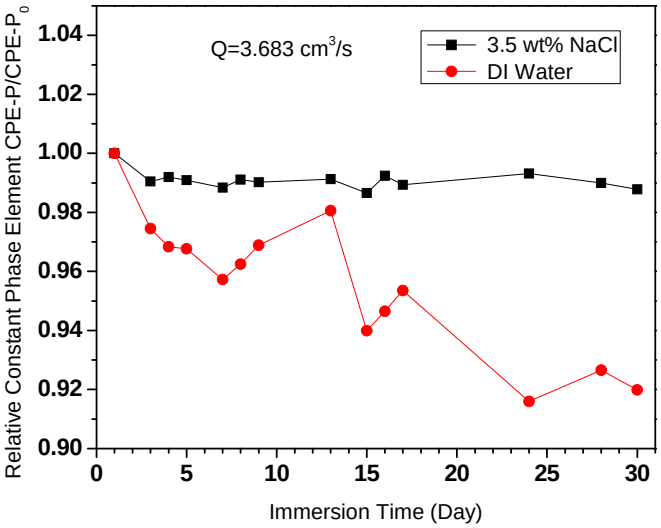

(b) Q=3.683 cm^3/s

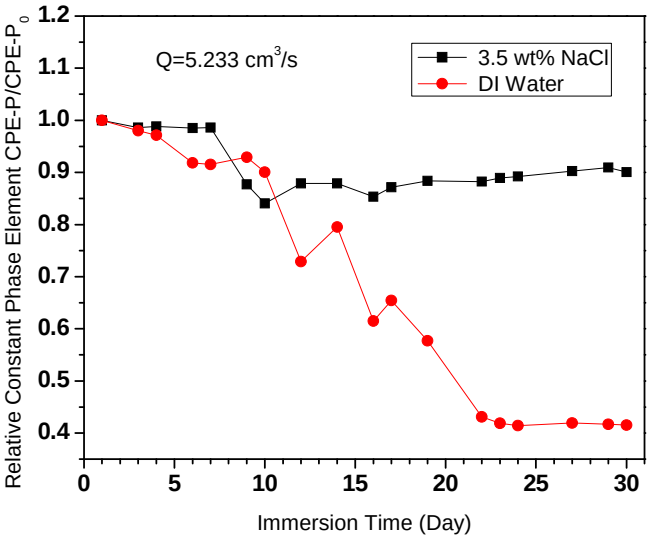

(c) Q=5.233 cm^3/s

Fig. 8. Relative constant phase element CPE-P as a function of immersion time for coated samples immersed in 3.5 wt% NaCl solution and DI water for flow rates Q=0 (stationary), 3.683, and 5.233 cm^3/s.

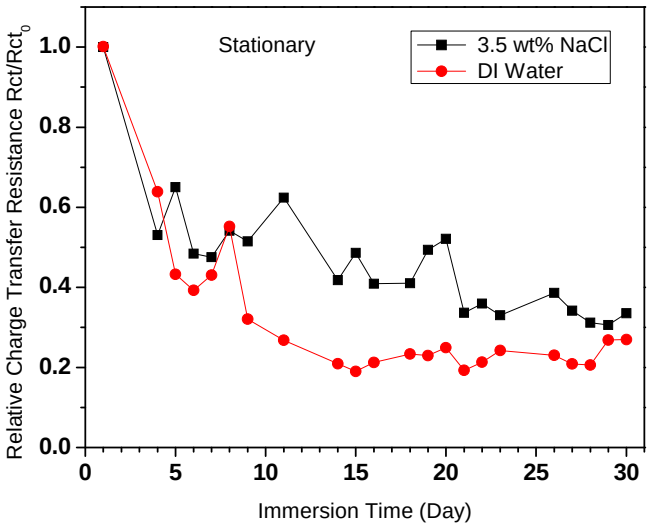

(a) Stationary immersion

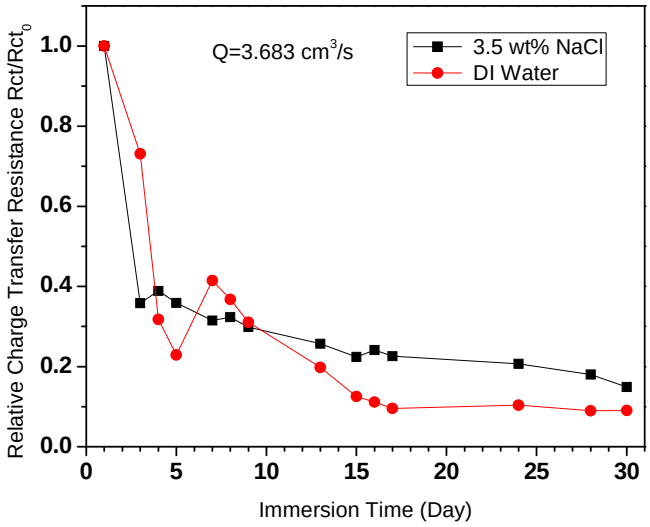

(b) Q=3.683 cm^3/s

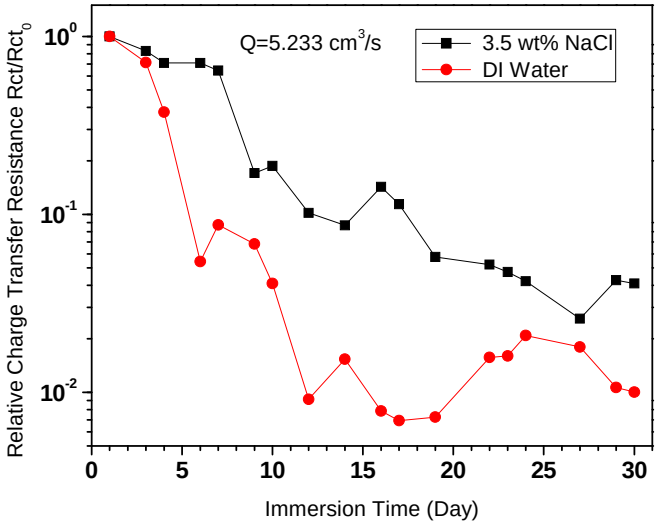

(c) Q=5.233 cm^3/s

Fig. 9. Relative charge transfer resistance as a function of immersion time for coated samples immersed in 3.5 wt% NaCl solution and DI water for flow rates Q=0 (stationary), 3.683, and 5.233 cm^3/s.

The behavior of physical elements (CPE-T, CPE-P, and R_{ct}) in the equivalent circuit model shows that DI water deteriorates the barrier properties of organic coatings more aggressively than 3.5 wt% NaCl solution. This would imply that the DI water is interacting spontaneously with coating components. The fact that the flowing DI water accelerates more aggressively the coating degradation may be explained by the large difference between the concentration of water soluble

substances released from the coating located in coating layers and that in the refreshing DI water over the coating surface. One of the evidence for the afore-mentioned large concentration difference may lie in the blistering of the coatings as discussed in section 3.3.

3.3 Topography Characterization

The change of the thickness of the organic coatings immersed in DI water is shown in Fig. 10. The coating thickness increases significantly after immersion in the flowing DI water, while it maintains almost the same in stationary immersion. This is because blisters (which can be seen by naked eyes) are generated on the coating surface after the immersion in flowing DI water. However, there is no obvious blistering on the coating surface after stationary immersion. On the contrary, the thickness of the organic coatings is found to decrease after immersion in the flowing 3.5 wt% NaCl solution (results not shown), and no major blistering has been observed for all flow conditions. The thickness is believed to be reduced by the abrasion of flowing NaCl solution. And the existence of blistering may explain the difference in thickness evolution between samples immersed in DI water and the NaCl solution.

The gloss of the coating surface is evaluated to quantify the roughness on the coating surface before and after immersion in DI water. Gloss reflects the smoothness of the surface. A mirror-like surface has a high gloss value, while a rough surface shows a lower one. The values obtained from the glossmeter indicate the percentage of the light reflection on the coating surface with respect to that on a black glass standard at three different grazing angles: 20˚, 60˚ and 85˚. The gloss measurements of the coatings are listed in Table 2. For all grazing angles, the gloss values are reduced after the immersion which implies that the surface becomes rougher due to blistering.

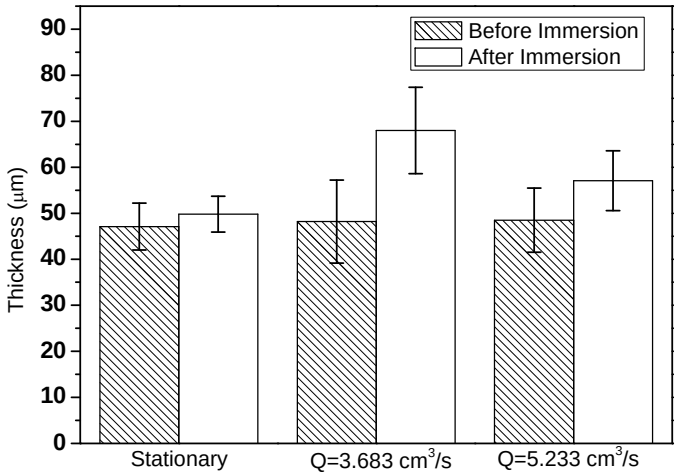

Fig. 10. Thickness of coated samples

immersed in DI water for flow rates Q=0 (stationary), 3.683, and 5.233 cm^3/s.

Table 2. Gloss measurements for coated samples

immersed in DI water for flow rates Q=0 (stationary), 3.683, and 5.233 cm^3/s

Immersion	Before Immersion			After Immersion		
Condition	20°	60°	85°	20°	60°	85°
Stationary	11.9 ± 1.7	43.0 ± 2.8	45.9 ± 2.9	9.7 ± 1.0	37.6 ± 1.2	42.0 ± 2.6
Q=3.683 cm^3/s	19.3 ± 4.7	45.9 ± 8.4	29.1 ± 7.5	5.4 ± 3.5	18.5 ± 9.3	13.2 ± 7.1
Q=5.233 cm^3/s	18.5 ± 5.3	57.3 ± 4.9	55.4 ± 4.5	8.3 ± 0.9	30.4 ± 0.8	35.7 ± 3.8

The optical microscopy images of the coating surface are presented in Fig. 11 for the coating before and after immersion in DI water. The surface is smooth before immersion. Under stationary immersion, DI water contributes little to modify the coating surface. However, after the immersion in flowing DI water, spherical protuberances appear on the coating surface. These protuberances could be the blisters connecting with each other. These images can verify the gloss measurement results that flowing condition contributes more to increase the surface roughness due to blistering. The blistering also results in the increasing coating thickness as well as the decreasing gloss.

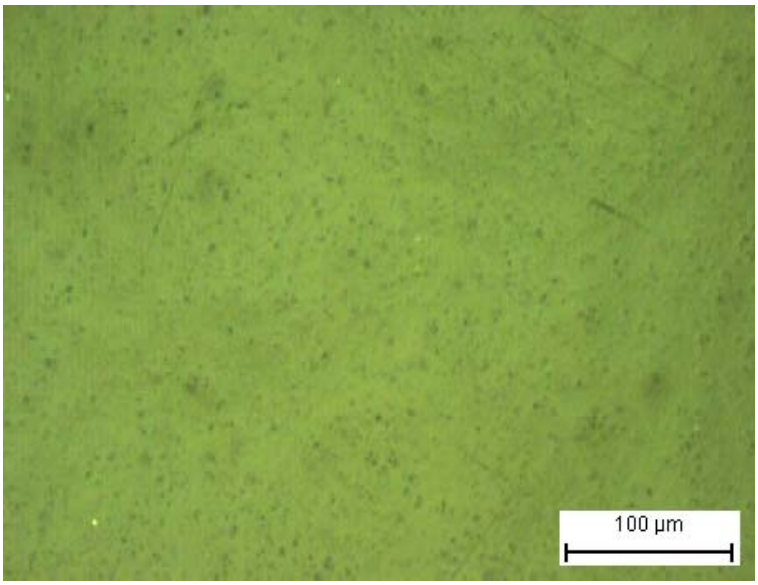

(a) Before degradation

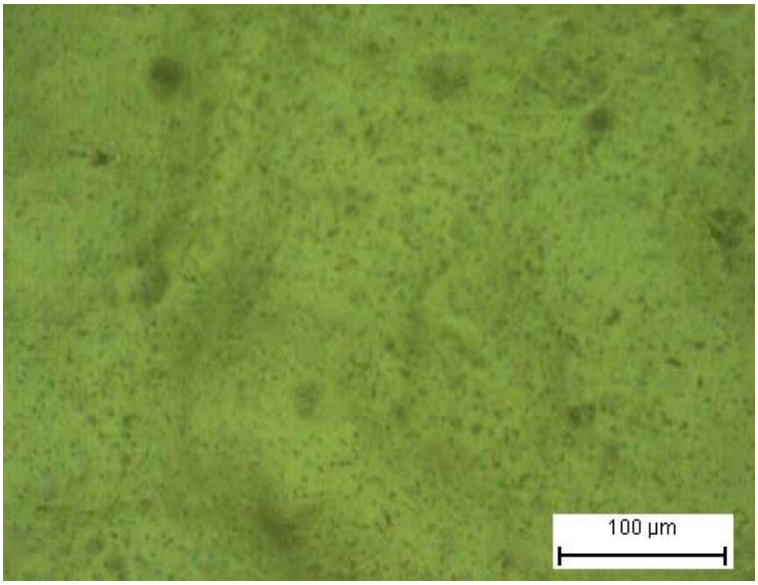

(b) After degradation under DI water stationary immersion

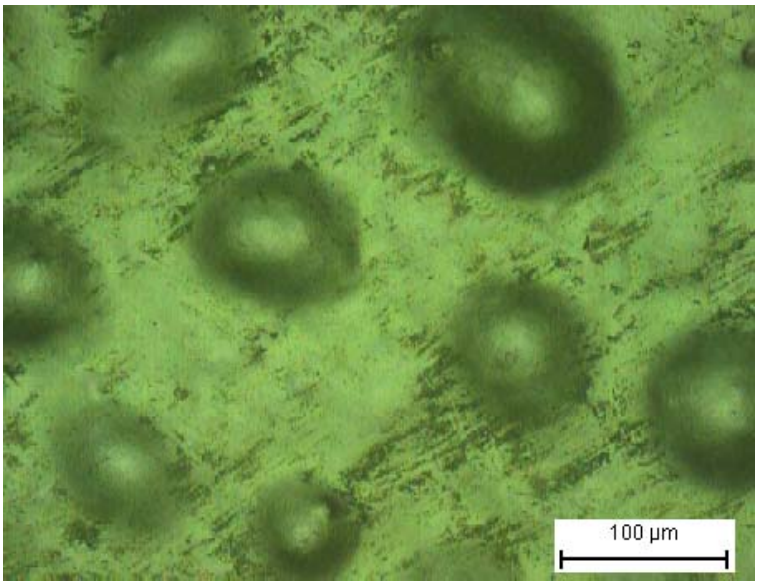

(c) After degradation with flow rate Q=3.683 cm^3/s

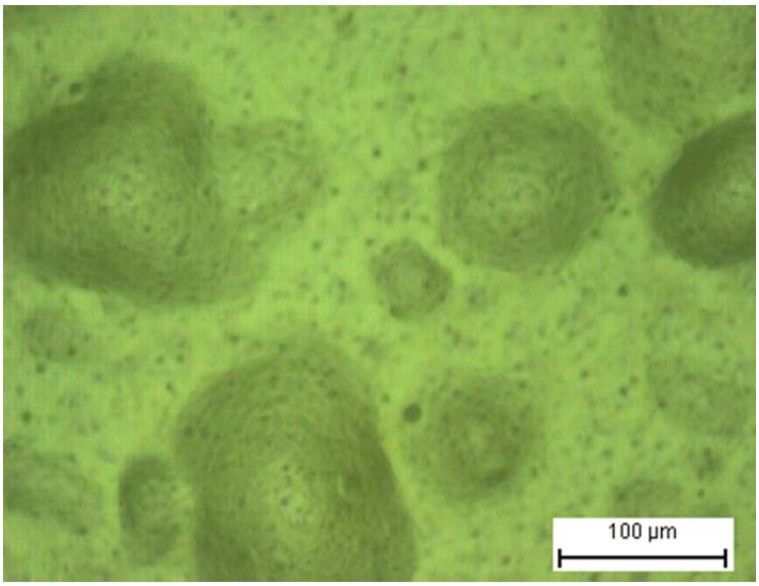

(d) After degradation with flow rate Q=5.233 cm^3/s

Fig. 11. Optical microscopy images of the coating surface before and after immersion.

Blistering is a common phenomenon in coating degradation representing the initial physical change due to alternating environments [47]. The formation of blistering is usually the first visible indication of insufficient protection by organic coating against corrosion [48]. Blistering may be caused by the permeation of water to coating metal interface due to osmotic pressure [9]. Our study shows that the flowing fluid over the coating surface promotes blistering to a more

severe level. We believe that soluble species (e.g. polar plasticizers and/or the non-cured polymer chain) may be diffusing out of the coating as water and ions percolate into the coating since mass loss of the coating and conductivity changes of the solution during the coating immersion has been reported in literature [46, 49]. Blistering promoted by flowing fluid may be explained by the fact that flowing DI water helps to maintain a large concentration difference of soluble species released from coatings between the coating layers and the bulk solution by constantly refreshing the fluid on the coating surface. Hence the osmotic pressure is maintained throughout the immersion which promotes the generation of blisters. On the contrary, for coatings in the stationary immersion, the ion concentration difference decreases due to the diffusion so that the osmotic effect diminishes as equilibrium is achieved. However, other factors may also influence the blistering of coatings in flowing DI water, such as the fluid shear exerted on the coating surface. Additional explanations may also be possible for the significant difference in the blistering behavior of coatings when immersed in flowing and stationary DI water. A more in-depth investigation will be carried out on this subject in the near future.

4. Conclusions

This study evaluates via EIS the electrochemical behavior of organic coating immersed in DI water with flow rate of Q=0, 3.683, and 5.233 cm^3/s. Experimental results as well as equivalent circuit modeling results for coatings in DI water with all three flow rates are compared with those for 3.5 wt% NaCl solution.

The impedance spectra of coatings decreases with the immersion time and the decrease is more substantial for flowing fluid at higher flow rate disregard of the fluid type. Equivalent circuit modeling of the EIS data shows higher capacitance and lower resistance under flowing immersion. The topography of the coating surface changes more substantially for higher flow rate. Thus flowing fluid brings much greater destruction to the coatings than the corresponding stationary condition. And this destruction is more aggressive under higher flow rate.

The decay of relative impedance modulus is larger for the organic coatings immersed in DI water, which demonstrates that this organic coating is more sensitive to the penetration of DI water than the 3.5 wt% NaCl solution. We also observe by comparing the values of physical elements in the equivalent circuit model that DI water deteriorates the barrier properties of organic coatings more aggressively. The differences in physical elements between the usages of these two working fluids are more substantial for higher flow rates. We conclude that the flowing fluid, especially DI water, over coating surface could be used as an effective acceleration method.

Acknowledgement

The authors acknowledge the support by NSF EPS-0447679 and NDSU Advance FORWARD program sponsored by NSF HRD-0811239. Qixin Zhou acknowledges the support of the Presidential Doctoral Graduate Fellowship of North Dakota State University.

References

[1] G.P. Bierwagen, The science of durability of organic coatings: a foreword, Prog. Org. Coat., 15 (1987) 179-195.

[2] G.P. Bierwagen, Reflections on corrosion control by organic coatings, Prog. Org. Coat., 28 (1996) 43-48.

[3] Q.L. Thu, G.P. Bierwagen, S. Touzain, EIS and ENM measurements for three different organic coatings on aluminum, Prog. Org. Coat., 42 (2001) 179-187.

[4] G.P. Bierwagen, D.E. Tallman, J. Li, L. He, C.S. Jeffcoate, EIS studies of coated metals in accelerated exposure, Prog. Org. Coat., 46 (2003) 149-158.

[5] G.P. Bierwagen, L. He, J. Li, L. Ellingson, D.E. Tallman, Studies of a new accelerated evaluation method for coating corrosion resistance - thermal cycling testing, Prog. Org. Coat., 39 (2000) 67-78.

[6] X. Yang, C. Vang, D.E. Tallman, G.P. Bierwagen, S.G. Croll, S. Rohlik, Weathering degradation of a polyurethane coating, Polym. Degrad. Stab., 74 (2001) 341-351.

[7] X. Yang, J. Li, S.G. Croll, D.E. Tallman, G.P. Bierwagen, Degradation of low gloss polyurethane aircraft coatings under UV and prohesion alternating exposures, Polym. Degrad. Stab., 80 (2003) 51-58.

[8] S. Touzain, Q.L. Thu, G. Bonnet, Evaluation of thick organic coatings degradation in seawater using cathodic protection and thermally accelerated tests, Prog. Org. Coat., 52 (2005) 311-319.

[9] J.H. Park, G.D. Lee, H. Ooshige, A. Nishikata, T. Tsuru, Monitoring of water uptake in organic coatings under cyclic wet-dry condition, Corros. Sci., 45 (2003) 1881-1894.

[10] F.X. Perrin, C. Merlatti, E. Aragon, A. Margaillan, Degradation study of polymer coating: Improvement in coating weatherability testing and coating failure prediction, Prog. Org. Coat., 64 (2009) 466-473.

[11] X. Jiang, Y. Zheng, W. Ke, Effect of flow velocity and entrained sand on inhibition performances of two inhibitors for CO_2 corrosion of N80 steel in 3% NaCl solution, Corros. Sci., 47 (2005) 2636-2658.

[12] A.S. Shehata, S.A. Nosier, G.H. Sedahmed, The role of mass transfer in the flow-induced corrosion of equipments employing decaying swirl flow, Chem. Eng. Process., 41 (2002) 659-666.

[13] J.A. Wharton, R.J.K. Wood, Influence of flow conditions on the corrosion of AISI 304L stainless steel, Wear, 256 (2004) 525-536.

[14] J. Villarreal, D. Laverde, C. Fuentes, Carbon-steel corrosion in multiphase slug flow and CO_2, Corros. Sci., 48 (2006) 2363-2379.

[15] L. Niu, Y. Cheng, Synergistic effects of fluid flow and sand particles on erosoin-corrosion of aluminum in ethylene glycol-water solutions, Wear, 265 (2008) 367-374.

[16] D. Zheng, D. Che, Y. Liu, Experimental investigation on gas-liquid two-phase slug flow enhanced carbon dioxide corrosion in vertical upward pipeline, Corros. Sci., 50 (2008) 3005-3020.

[17] L. Xu, Y. Cheng, Effect of fluid hydrodynamics on flow-assisted corrosion of aluminum alloy in ethylene glycol-water solution studied by a microelectrode technique, Corros. Sci., 51 (2009) 2330-2335.

[18] Y.P. Purandare, M.M. Stack, P.E. Hovsepian, Velocity effects on erosion-corrosion of CrN/NbN "superlattice" PVD coatings, Surf. Coat. Technol., 201 (2006) 361-370.

[19] E. Heitz, Mechanistically based prevention strategies of flow-induced corrosion, Electrochim. Acta, 41 (1996) 503-509.

[20] K. Ranjbar, Effect of flow induced corrosion and erosion on failure of a tubular heat exchanger, Mater. Des., 31 (2010) 613-619.

[21] J. Tu, The effect of TiN coating on erosion-corrosion resistance of α-Ti alloy in saline slurry, Corros. Sci., 42 (2000) 147-163.

[22] S.S. Rajahram, T.J. Harvey, R.J.K. Wood, Erosion-corrosion resistance of engineering materials in various test conditions, Wear, 267 (2009) 244-254.

[23] M. Bjordal, E. Bardal, T. Rogne, T.G. Eggen, Erosion and corrosion properties of WC coatings and duplex stainless steel in sand-containing synthetic sea water, Wear, 186-187 (1995) 508-514.

[24] M.M. Stack, T.M. Abd El Badia, Mapping erosion-corrosion of WC/Co-Cr based composite coatings: Particle velocity and applied potential effects, Surf. Coat. Technol., 201 (2006) 1335-1347.

[25] R.A. Cottis, L.L. Shreir, Shreir's Corrosion, Elsevier, Amsterdam, London, 2010.

[26] V. Barranco, S. Feliu, EIS study of the corrosion behaviour of zinc-based coatings on steel in quiescent 3% NaCl solution. Part 1: directly exposed coatings, Corros. Sci., 46 (2004) 2203-2220.

[27] F. Rezaei, F. Sharif, A.A. Sarabi, S.M. Kasiriha, M. Rahmaniam, E. Akbarinezhad, Evaluating water transport through high solid polyurethane coating using the EIS method, J. Coat. Technol. Res., 7 (2010) 209-217.

[28] M. Del Grosso Destreri, J. Vogelsang, L. Fedrizzi, F. Deflorian, Water up-take evaluation of new waterborne and high solid epoxy coatings. Part II: electrochemical impedance spectroscopy, Prog. Org. Coat., 37 (1999) 69-81.

[29] C.S. Jeffcoate, G.P. Bierwagen, Electrochemical comparison of coating performance in flowing vs. stationary electrolyte, in: G.P. Bierwagen (Ed.) American Chemical Society Symposium Series, American Chemical Society, Washington, DC, 1998, pp. 151-160.

[30] Y. Wei, L. Zhang, W. Ke, Comparison of the degradation behaviour of fusion-bonded epoxy powder coating systems under flowing and static immersion, Corros. Sci., 48 (2006) 1449-1461.

[31] Y. Wang, G.P. Bierwagen, A new acceleration factor for the testing of corrosion protective coating: flow-induced coating degradation, J. Coat. Technol. Res., 6 (2009) 429-436.

[32] T. Hodgkiess, D. Mantzavinos, Corrosion of copper-nickel alloys in pure water, Desalination, 126 (1999) 129-137.

[33] D. Mantzavinos, T. Hodgkiess, S.L.C. Lai, Corrosion of condenser tube materials in distilled water, Desalination, 138 (2001) 365-370.

[34] Z. Lu, T. Shoji, Y. Takeda, Y. Ito, A. Kai, S. Yamazaki, Transient and steady state crack growth kinetics for stress corrosion cracking of a cold worked 316L stainless steel in oxygenated pure water at different temperatures, Corros. Sci., 50 (2008) 561-575.

[35] C.R. Alentejano, I.V. Aoki, Localized corrosion inhibition of 304 stainless steel in pure water by oxyanions tungstate and molybdate, Electrochim. Acta, 49 (2004) 2779-2785.

[36] L. Liu, Y. Li, C. Zeng, F. Wang, Electrochemical impedance spectroscopy (EIS) studies of the corrosion of pure Fe and Cr at 600 °C under solid NaCl deposit in water vapor, Electrochim. Acta, 51 (2006) 4736-4743.

[37] B.R. Hinderliter, S.G. Croll, D.E. Tallman, Q. Su, G.P. Bierwagen, Interpretation of EIS data from accelerated exposure of coated metals based on modeling of coating physical properties, Electrochim. Acta, 51 (2006) 4505-4515.

[38] R. Cottis, S. Turgoose, Electrochemical Impedance and Noise, NACE International, Houston, 1999.

[39] Q. Zhou, Y. Wang, X. Qu, G.P. Bierwagen, Influence of immersion condition on organic coating degradation in deionized water and electrolyte solution, to be submitted.

[40] J.R. Davis, Corrosion Understanding the Basics, ASM International, 2000.

[41] H. Hu, N. Li, J. Cheng, L. Chen, Corrosion behavior of chromium-free dacromet coating in seawater, J. Alloys Compd., 472 (2009) 219-224.

[42] F. Wong, R.G. Buchheit, Utilizing the structural memory effect of layered double hydroxides for sensing water uptake in organic coatings, Prog. Org. Coat., 51 (2004) 91-102.

[43] A. Peyman, C. Gabriel, E.H. Grant, Complex permittivity of sodium chloride solutions at microwave frequencies, Bioelectromagnetics, 28 (2007) 264-274.

[44] J. Hu, J. Zhang, C. Cao, Determination of water uptake and diffusion of Cl^- ion in epoxy primer on aluminum alloys in NaCl solution by electrochemical impedance spectroscopy, Prog. Org. Coat., 46 (2003) 273-279.

[45] X. Yang, D.E. Tallman, S.G. Croll, G.P. Bierwagen, Morphological changes in polyurethane coatings on exposure to water, Polym. Degrad. Stab., 77 (2002) 391-396.

[46] A.S.L. Castela, A.M. Simões, M.G.S. Ferreira, E.I.S. evaluation of attached and free polymer films, Prog. Org. Coat., 38 (2000) 1-7.

[47] X. Yang, D.E. Tallman, G.P. Bierwagen, S.G. Croll, S. Rohlik, Blistering and degradation of polyurethane coatings under different accelerated weathering tests, Polym. Degrad. Stab., 77 (2002) 103-109.

[48] W. Funke, Blistering of paint films and filiform corrosion, Prog. Org. Coat., 9 (1981) 29-46.

[49] N. Fredj, S. Cohendoz, S. Mallarino, X. Feaugas, S. Touzain, Evidencing antagonist effects of water uptake and leaching processes in marine organic coatings by gravimetry and EIS, Prog. Org. Coat., 67 (2010) 287-295.